Int J Clin Exp Med 2017;10(1):426-433
www.ijcem.com /ISSN:1940-5901/IJCEM0021589

Original Article

Homing of SPIO-MSCs to liver metastasis in nude mice

Huan Li[1], Jie Tian[2], Jin-Hua Cai[1], He-Lin Zheng[1], Kun Zhu[1], Chuan Feng[1]

[1]Department of Radiology, Children's Hospital, Chongqing Medical University, Chongqing, China; [2]Key Laboratory of Diagnostic Medicine Designated by The Chinese Ministry of Education, School of Diagnostic Medicine, Chongqing Medical University, Chongqing, China

Received December 10, 2015; Accepted March 19, 2016; Epub January 15, 2017; Published January 30, 2017

Abstract: Objective: This study aims to investigate the feasibility of delivering SPIO (full name?) to tumor metastases through homing of mesenchymal stem cells (MSCs). Methods: The effect on MSCs activity by various concentrations of SPIO and the acquired ion level at each concentration were detected by ??. The in vitro migration ability of SPIO labeled MSCs (SPIO-MSCs) toward C6 glioma was detected by Transwell assay. PBS control, SPIO and SPIO-MSCs were respectively injected into the tail vein of nude mice glioma xenograft models with hepatic metastases. On the 9th day after injection, liver tumors were scanned by 7.0T MR, and the corresponding T2WI, T2 signal strength and T2* values were detected. The pathological samples were sectioned and stained by Prussian blue to detect labeled MSCs. Results: Labeled with 160 μg/ml SPIO did not affect MSCs cellular activity. Transwell experiment demonstrated that SPIO-MSCs kept the migration ability toward C6 glioma. The MR T2WI signal of tumor nodules of SPIO-MSCs injected group was significantly decreased compared with the other two groups. And the T2 signal strength and T2* value of SPIO-MSCs injected group were both reduced compared to the other two groups. SPIO-MSCs were detected in the tumor region in SPIO-MSCs injected group by Prussian blue staining. Conclusion: MSCs are able to deliver SPIO to hepatic tumor metastases by homing.

Keywords: Mesenchymal stem cell, homing, tumor metastasis, superparamagnetic iron oxide (SPIO)

Introduction

SPIO is a super paramagnetic substance, mainly composed of Fe_4O_3 and γ-Fe_2O_3, which is simply prepared by co-precipitation, hydrothermal reactions, sol-gel process, etc. The prepared SPIO can decrease the MR T2 relaxation time, lead to a low T2WI signal of the surrounding tissues and decrease T2 relaxation time, making SPIO a good contrast agent for MR in clinical studies. Studies have demonstrated that using SPIO to label cells will not affect cell activity or differentiation, thus SPIO labeling can be used for in vivo tracking. MR imaging of stem cells after SPIO labeling is emerging as a specific target cell detection technique, which can observe the in vivo distribution and survival of stem cells after transplantation in a real-time fashion, playing an important role in the evaluation of stem cell transplantation effect and the optimization of stem cell transplantation treatment protocol [1]. The safety and high efficiency of using SPIO for stem cells labeling are critical for studies of MR in vivo tracking. At present, the commonly used methods are transfection agent method and SPIO-SiO2-FITC, which enters the cells by phagocytosis. In addition, SPIO is able to produce heat under alternating magnetic field, exhibiting great potential in killing tumor cells by magnetic hyperthermia.

Mesenchymal stem cells (MSCs) are pluripotent stromal cells that do not belong to hematopoietic tissues. Due to the advantages such as easy isolation and culture, multipotency, paracrine effects and immunomodulatory effects, MSCs have been considered as the most promising stem cells for the treatment of a variety of disease. MSCs homing, similar to lymphocytes homing, refers to the process during which the endogenous or exogenous MSCs migrate directionally towards and engraft into the target tissue under the influences of various factors [2-4]. A number of studies about MSCs homing have shown that the detection rate of implanted MSCs in the target tissues is very low, which affects target tissue repair by MSCs [5, 6]. This may be related to MSCs survival in target tis-

sues. Another important factor is the low ratio of injected MSCs penetrating the blood vessels and selectively reaching the target tissues and engrafting [7]. Therefore, MSCs homing has become the key step in MSCs treatment and been widely concerned. It has been demonstrated that a variety of tumor cells can cause the directional migration of MSCs [8-10]. Directional migration of MSCs towards tumor cells, namely MSCs homing, is similar to the mechanism of leukocyte directional migration towards inflammatory tissues (including the participating molecules such as chemokines and receptors, as well as adhesion molecules) [11-13]. In most previous studies of MSCs homing, in situ tumors were established by local injections, thus there was interference from tissue injury at the tumor site [14, 15].

The nude mice xenograft model with liver hematogenous metastases established in this study avoided the interference from tissue injury at the tumor site, which was proved to be more consistent with the actual physiological condition of tumor metastases. We also used SPIO to label MSCs, and SPIO was successfully delivered by MSCs homing to liver hematogenous metastases, ultimately leading to the MR signal change of tumor. This study may provide reference for the early discovery of tumor metastasis and also provide a basis for further studies about magnetic hyperthermia treatment of tumor metastasis.

Material and methods

SPIO labeling MSCs and iron quantification

Nude mice were acquired from the animal center at Chongqing College of Medicine and approved by Animal Ethics Committees, which were anesthetized. The femur and tibia bones were isolated under sterile conditions. MSCs were obtained after marrow cavity wash. The MSCs were cultured at 37°C with 5% CO_2, and regular media change and passage were conducted. From the 3rd generation, MSCs were collected and used for experiments.

Different concentrations of SPIO (20 μg/ml, 40 μg/ml, 80 μg/ml, 120 μg/ml and 160 μg/ml) were prepared by mixing DMEM/F12 (Gibco, USA), liposomes (LipoFiter™ Hanheng Bio, Shanghai) and SPIO (Wande Hitech, Beijing) following different ratios. The DMEM/F12 containing SPIO was added to MSCs. Cells were co-cultured for 6 h and washed with PBS until PBS solution turned clear. Cells were digested by pancreatic enzymes and counted using automated cell counter (Count Star, Shanghai China). Cells were centrifuged and incubated in 1 M HCl overnight. After dilution, the iron level in each cell at different SPIO concentration was detected on atomic absorption spectroscopy.

Detection of the effect of different concentrations of SPIO on cell activity using CCK-8

MSCs were seeded in a 96-well plate, with 4000 cells per well (6 replicate wells for each group). Cells were cultured at 37°C, with 5% CO_2 in an incubator for 24 h. MSCs were transfected with various concentrations of SPIO following the method aforementioned. 6 h later, cells were taken out of the incubator for media change. MSCs were washed with PBS twice, and added with DMEM/F12 100 μl/well and CKK-8 solution (Dojindo, Japan) 10 μl/well. 2 h later, OD value was detected at 450 nm by spectrophotometer.

Prussian blue staining of SPIO-MSCs and TEM detection

SPIO labeled MSCs were treated with paraformaldehyde and 0.5% Triton X-100c. Prussian blue was added for staining for 5 min. Cells were observed under the inverted microscope and 10 regions were randomly selected for cell counting. The staining ratio of MCSs was calculated.

SPIO-MSCs were digested by pancreatic enzymes and centrifuged at 1200 rpm for 10 min. The supernatant was discarded. Cells were fixed using glutaraldehyde. After dehydration, embedment, trimming and sectioning, cells were observed under a transmission electron microscope (H-7500, Hitachi, Japan).

Transwell invasion assays

200 μl (10^5 cells) media containing MCSs and SPIO-MCSs (SPIO transfection concentration 160 μg/ml) were plated in the 8 μm upper well of Transwell plate (Corning), respectively. 2 ml of DMEM/F12 and DMEM/F12 containing C6 (10^6 cells) were added in the bottom well. 24 h later, the MSCs in the upper well which failed to pass the pore were wiped off carefully by

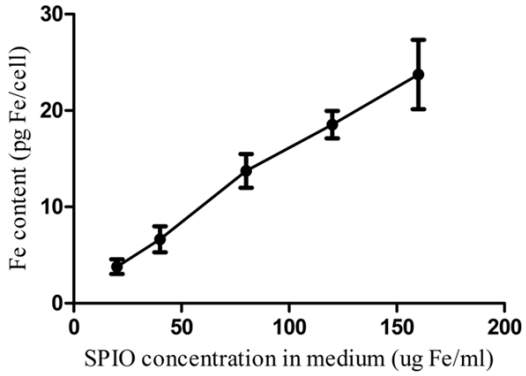

Figure 1. Iron Level of SPIO-MSCs under different SPIO transfection concentration.

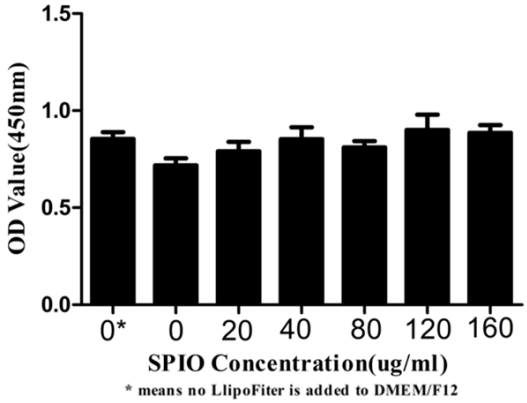

Figure 2. Cell activity detection of SPIO-MSCs.

sterile cotton stick. After crystal violet staining, cells were observed using inverted microscope and 10 viewing regions were selected randomly for cell counting.

Construction of liver hematogenous metastases of glioma model and injection of SPIO-MSCs

C6 glioma cells were thawed, cultured and passaged following the regular methods. Cells at logarithmic phase were collected, digested by pancreatic enzymes, centrifuged and counted. Cell concentration was adjusted to 1×10^7/ml by PBS. 9 male mice were selected and the hepatic portal vein was exposed by surgery. 0.1 ml cell suspension was injected into the nude mice hepatic portal vein. Hemostasis was done by finger pressing and the incision was sewn up. Nude mice were placed back to the cages and raised after surgery. The 9 nude mice were divided randomly into 3 groups. SPIO at a concentration of 160 μg/ml was used to label MSCs. On the 7th day after modeling, unlabeled MSCs (10^6 cells), SPIO-MSCs (10^6 cells) and SPIO (50 μg) were injected into nude mouse tail vein, respectively.

7.0T MR scanning of liver tissue of nude mouse xenograft

MSCs, SPIO-MSCs and SPIO were injected into the tail vein of the nude mouse xenograft, respectively. On the 9th day after injection, nude mice were anesthetized by ether and placed within 7.0T BioSpec70/20USR coil.

The parameters are listed as follows:

T2WI sequence: TR = 2000 ms; TE = 30 ms; ECHO SPACING = 15 ms; Repetitions = 1; field of view = 40*40; Image size = 256*256; T2*WI sequence: TR = 1000 ms; TE = 4.5 ms; Flip angle = 50°, echo images = 8; Repetitions =1; field of view = 40*40; Image size = 256*256.

Tumor metastasis nodules and normal liver tissues were randomly selected from the MRI images of liver scanning of the 9 nude mouse models (9 metastasis nodules and 9 normal liver tissues were selected from each nude mouse). T2 signal strength and T2* value were calculated using ParaVision 6.0 software.

Prussian blue staining of liver of nude mouse xenograft

After MR scanning, liver tissues of nude mice were fixed by 4% paraformaldehyde, dehydrated, embedded in paraffin, cut into 4 μm sections, dewaxed, and re-hydrated. Prussian blue was dropped onto tissue slides for 15 min staining. Prussian blue was washed off and hematoxylin was added for 5 min staining. Tissue was mounted using neutral gum and observed under inverted microscope.

Results

Iron level detection in SPIO-MSCs

MSCs were labeled with SPIO in a gradient concentration of 20 μg/ml, 40 μg/ml, 80 μg/ml, 120 μg/ml and 160 μg/ml by liposome mediated method. 6 h after co-culture, the acquired iron level under each condition was detected using atomic absorption spectrometer. Results are shown in **Figure 1**.

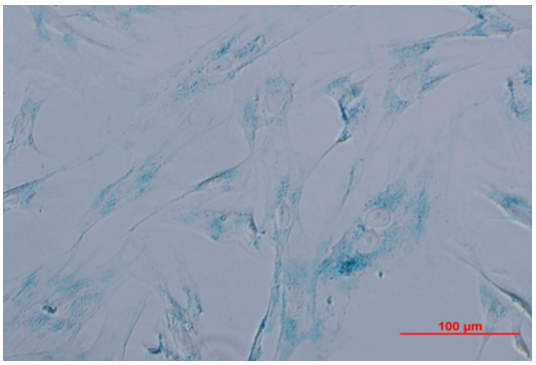

Figure 3. SPIO-MSCs Prussian blue staining.

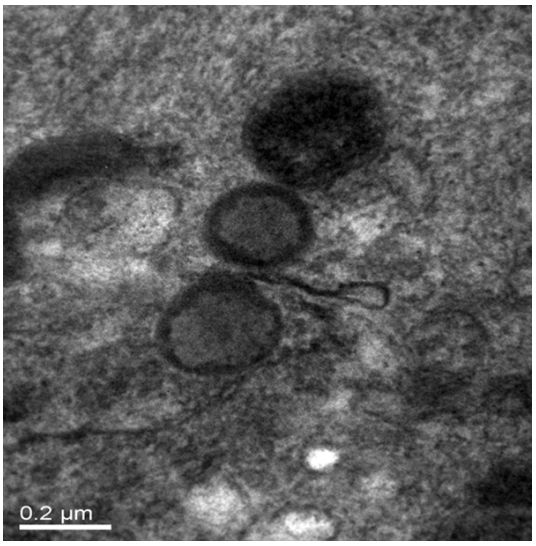

Figure 4. TEM of SPIO-MSCs (×80000).

Table 1. Cell counts of MSCs and SPIO-MSCs in transwell assay

	MSCs	SPIO-MSCs
C6	63	61
0	23	19

The results showed that the iron level in SPIO-MSCs increased with increased concentration of SPIO added in the co-culture media, with a positive correlation. At an SPIO concentration of 160 μg/ml, the iron level in SPIO-MSCs was 23.73±3.59 pg/cell.

Effect on cell activities by different concentrations of SPIO

The influence of SPIO at various concentrations on MSCs cell activity was detected through the OD450 nm value of each well after SPIO transfection using CCK-8 by microplate reader. The results are shown in **Figure 2**.

The OD value under each SPIO concentration was analyzed by one-way ANOVA. The difference between each SPIO labeling concentration was statistically insignificant ($P > 0.05$). Thus, SPIO was not considered to affect cell activity at a high concentration.

Prussian blue staining of SPIO-MSCs and TEM detection results

After Prussian blue staining, SPIO labeled MSCs were observed under inverted microscope. 10 viewing regions were randomly selected for cell counting and SPIO labeling ratio calculation. Detailed results are shown in **Figure 3**.

The results of each viewing field under inverted microscope showed that, all SPIO-MSCs were stained into blue color after Prussian blue treatment. Blue particles were observed around the central large round nucleus at high density in the cytoplasm, while not seen in the nucleus. After cell counting, the cell transfection ratio was 100%, indicating a high successful transfection ratio by using this method to transfect MSCs.

The labeled SPIO-MSCs were digested by pancreatic enzymes, centrifuged, fixed, dehydrated, embedded, trimmed, sectioned and observed under TEM. Results are shown in **Figure 4**.

Results of TEM showed that there were like-round phagosomes in the cytoplasm of SPIO-MSCs, with a diameter of 200 nm. Small dense particles were distributed in the phagosomes. SPIO particles not engulfed by MSCs were also observed. The results showed that MSCs were successfully labeled by SPIO in this approach.

Results of transwell experiment

In the Transwell assay, cells were stained by crystal violet and observed under inverted microscope. 10 viewing fields were selected randomly for MSCs and SPIO-MSCs counting. Results are shown in **Table 1**.

As shown by the MSCs and SPIO-MSCs cell counting results in the Transwell assay, SPIO-

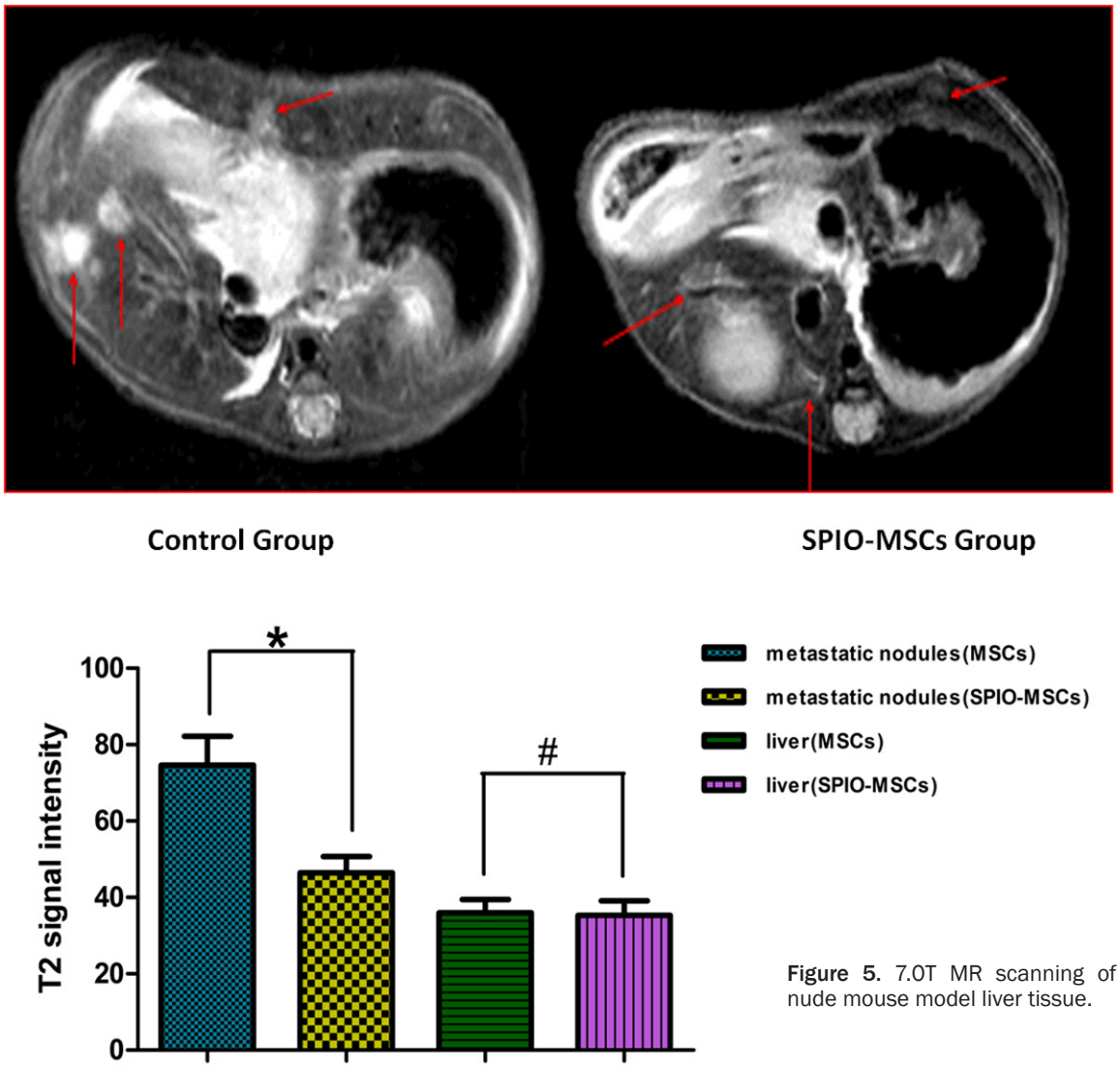

Figure 5. 7.0T MR scanning of nude mouse model liver tissue.

MSCs successfully invaded and migrated through homing activity.

Results of 7.0T MR scanning

MSCs, SPIO-MSCs and SPIO were injected into the tail vein of the nude mouse xenograft, respectively. On the 9th day after injection, nude mice were anesthetized by ether and placed within 7.0T BioSpec70/20USR coil. Liver tissues of the 9 nude mouse models were scanned and MRI images were obtained. Tumor metastasis nodules and normal liver tissues were randomly selected. T2 signal strength and T2* value were calculated using ParaVision 6.0 software. The results are shown in **Figure 5**.

The 7.0T MR scanning of experimental nude mouse liver tissues revealed that the control metastasis signal was high, while metastasis signal of SPIO-MSCs group was low. In tumor metastatic nodules, T2 signal of MSCs was higher than that of SPIO-MSCs. In normal liver tissues, the T2 signals in the two groups were comparable. The SPIO-MSCs injected in the tail vein of the nude mouse model successfully homed and migrated to the liver metastatic nodules, and exerted its therapeutic effect.

Results of Prussian blue staining of liver tissue of nude mouse xenograft

After MR scanning, the liver tissues of experimental nude mice were fixed, dehydrated, embedded, sectioned, de-waxed, rehydrated and stained by Prussian blue. Tissues were observed under inverted microscope and results are shown in **Figure 6**.

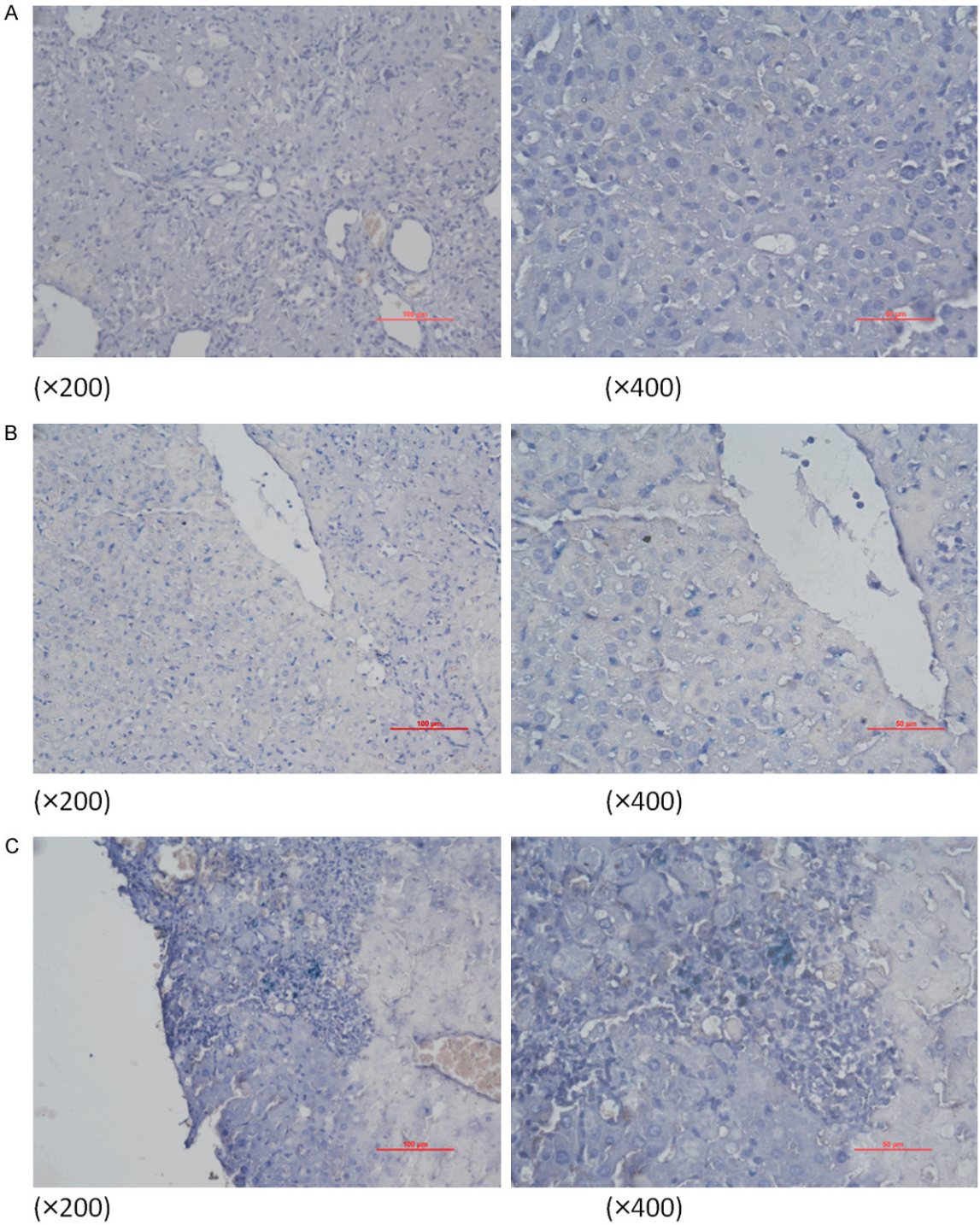

Figure 6. Prussian blue staining of liver tissue of nude mouse model. A. Control Group; B. SPIO Injection Group; C. SPIO-MSCs Injection Group.

The results of Prussian blue staining of the liver tissue from the nude mouse model showed that in control group, stained cells were not observed in either tumor site or normal liver tissue. In SPIO injection group, blue stained cells were evenly distributed in normal liver tissues, which presumably might be the macrophages engulfing SPIO (kuffer cells). However, the blue stained cells were not observed at tumor site, and it was possibly because the tumor region

formed by C6 glioma cells didn't contain macrophages (kuffer cells), which was not able to engulf exogenous SPIO to exhibit blue color. The blue stained cells observed in the tumor sites in SPIO-MSCs injection group were the SPIO-MSCs labeled in vitro, while blue stained SPIO-MSCs were not observed in normal liver tissues. The injected SPIO-MSCs were able to directionally home to the tumor region in liver tissues of the nude mouse xenograft.

Discussion

The MR tracking and stem cell labeling by SPIO enable non-invasive monitoring of biological activity of in vivo transplantation of stem cells. However, this new approach still faces many problems, such as cytoplasmic iron dilution by cell division, engulfment of dead labeled cells by macrophages, or metabolism and elimination of iron in undivided cells. It needs further investigation on whether these conditions will cause non-specific signal reduction in the MR image and interfere with the specificity of survived labeled cells [16, 17]. Cao et al. [18] demonstrated the feasibility of tracking rabbit disc degeneration using SPIO labeled rabbit MSCs, and found that SPIO was able to effectively track MSCs transplanted into the discs. Histology study confirmed that extracellular matrix of nucleus pulposus cells was increased and disc degeneration was slowed down after transplantation. Li et al. [19] demonstrated the feasibility of in vivo MR tracking by using SPIO labeled endothelial progenitor cells.

In this study, hematogenous metastasis model was established in nude mouse liver. Labeled by SPIO, MSCs delivered SPIO by homing to the liver hematogenous tumor metastases and ultimately reduced the MR signal strength of tumor sites, thus exerting a therapeutic effect. Transwell invasion assay is an experiment applying Transwell technique in tumor cell invasion study, but is not equal to invasion assay. There are various models and approaches in tumor cell invasion assays. Future studies may explore other methods to further confirm SPIO-MSCs homing to tumor metastases. A number of studies have shown that the homing action of stem cells towards injuries or ischemic tissues, as well as a series of molecules involved in this process, is very similar to the mechanism of leukocytes homing towards inflammatory tissues [20]. Although the mechanism of leukocytes homing to inflammatory tissue is clear, the specific mechanisms of stem cells homing to the injury or ischemic tissues remain unclear. The efficacy of MSCs methods can only be guaranteed by reaching a certain homing ratio. The low homing efficiency of MSCs is closely related with the unclear mechanism. At present many measures have been shown to promote MSCs homing. In-depth genetic and molecular study of these measures might be helpful in understanding MSCs homing mechanism to improve MSCs therapeutic spectrum and efficacy of MSCs. A few steps may effectively enhance the homing effect of MSCs toward target tissues. A good culture condition can help to maintain and even enhance the activity of MSCs. Stolzing et al. [21] discovered that culturing MSCs in low oxygen significantly reduced the accumulation of intracellular oxidative damage. Sotiropoulou et al. [22] found that low sugar DMEM, Gluramax and low density media might be more helpful for applying MSCs in cell therapy. MSCs adhesion prior to transplantation was found to facilitate MSCs survival after transplantation and homing to target tissues. The results of this study can provide reference for the early discovery of tumor metastasis and also provide a basis for future studies of magnetic hyperthermia treatment of tumor metastasis.

Acknowledgements

This work was supported by the National Natural Science Foundation of China (Grant Number: 81201744).

Disclosure of conflict of interest

None.

Address correspondence to: Dr. Chuan Feng, Department of Radiology, Children's Hospital, Chongqing Medical University, Chongqing, China. Tel: +86-2987767654; Fax: +86-2987767654; E-mail: fengchuan023@yeah.net

References

[1] Li ZF, Liu L, Tian W. MR Tracking of transplanted neural stem cells labeled with spio nanoparticles in rat brain after facial nerve injury. Chinese Journal of Medical Imaging Technology 2009; 25: 1941-1944.

[2] Bhakta S, Hong P, Koc O. The surface adhesion molecule CXCR4 stimulates mesenchy-

mal stem cell migration to stromal cell-derived factor-1 in vitro but does not decrease apoptosis under serum deprivation. Cardiovasc Revasc Med 2006; 7: 19-24.
[3] Schenk S, Mal N, Finan A. Monocyte chemotactic protein-3 is a myocardial mesenchymal stem cell homing factor. Stem Cells 2007; 25: 245-251.
[4] Cheng Z, Ou L, Zhou X, Li F, Jia X, Zhang Y, Liu X, Li Y, Ward CA, Melo LG, Kong D. Targeted migration of mesenchymal stem cells modified with CXCR4 gene to infarcted myocardium improves cardiac performance. Mol Ther 2008; 16: 571-579.
[5] Dhinsa BS, Adsida AB. Current clinical therapies for cartilage repair, their limitation and the role of stem cells. Curr Stem Cell Res Ther 2012; 7: 143-148.
[6] Segers VF, Van Riet I, Andries LJ, Lemmens K, Demolder MJ, De Becker AJ, Kockx MM, De Keulenaer GW. Mesenchymal stem cell adhesion to cardiac microvascular endothelium: activators and mechanisms. Am J Physiol Heart Circ Physiol 2006; 290: 1370-1377.
[7] Kyriakou C, Rabin N, Pizzey A, Nathwani A, Yong K. Factors that influence short-term homing of human bone marrow-derived mesenchymal stem cells in a xenogeneic animal model. Haematologica 2008; 93: 1457-1465.
[8] Dong F, Harvey J, Finan A, Weber K, Agarwal U, Penn MS. Myocardial CXCR4 expression is required for mesenchymal stem cell mediated repair following acute myocardial infarction. Circulation 2012; 126: 314-324.
[9] Freyman T, Polin G, Osman H, Crary J, Lu M, Cheng L, Palasis M, Wilensky RL. A quantitative, randomized study evaluating three methods of mesenchymal stem cell delivery following myocardial infarction. Eur Heart J 2006; 27: 1114-1122.
[10] Kitaori T, Ito H, Schwarz EM, Tsutsumi R, Yoshitomi H, Oishi S, Nakano M, Fujii N, Nagasawa T, Nakamura T. Stromal cell-derived factor 1/CXCR4 signaling is critical for the recruitment of mesenchymal stem cells to the fracture site during skeletal repair in a mouse model. Arthritis Rheum 2009; 60: 813-823.
[11] Schu S, Nosov M, O'Flynn L, Shaw G, Treacy O, Barry F, Murphy M, O'Brien T, Ritter T. Immunogenicity of allogeneic mesenchymal stem cells. J Cell Mol Med 2012; 16: 2094-2103.
[12] Hashemi SM, Ghods S, Kolodgie FD, Parcham-Azad K, Keane M, Hamamdzic D, Young R, Rippy MK, Virmani R, Litt H, Wilensky RL. A placebo controlled, dose-ranging, safety study of allogenic mesenchymal stem cells injected by endomyocardial delivery after an acute myocardial infarction. Eur Heart J 2008; 29: 251-259.
[13] Karp JM, Leng Teo GS. Mesenchymal stem cell homing: the devil is in the details. Cell Stem Cell 2009; 4: 206-216.
[14] Steingen C, Brenig F, Baumgartner L, Schmidt J, Schmidt A, Bloch W. Characterization of key mechanisms in transmigration and invasion of mesenchymal stem cells. J Mol Cell Cardiol 2008; 44: 1072-1084.
[15] Belema-Bedada F, Uchida S, Martire A, Kostin S, Braun T. Efficient homing of multipotent adult mesenchymal stem cells depends on FROUNT-mediated clustering of CCR2. Cell Stem Cell 2008; 2: 566-575.
[16] Xu L, Meng F, Ni M, Lee Y, Li G. N-cadherin regulates osteogenesis and migration of bone marrow-derived mesenchymal stem cells. Mol Biol Rep 2013; 40: 2533-2539.
[17] Rüster B, Göttig S, Ludwig RJ, Bistrian R, Müller S, Seifried E, Gille J, Henschler R. Mesenchymal stem cells display coordinated rolling and adhesion behavior on endothelial cells. Blood 2006; 108: 3938-3944.
[18] Cao Y, Wu XT, Wang YT. Study of in vivo Tracking of Bone Marrow Mesenchymal Stem Cells and the Treatment of Disc Degeneration. Journal of Southeast University 2009; 28: 269-273.
[19] Li CS, Kent DL, Chang KH, Padgett KR, Afzal A, Chandra SB, Caballero S, English D, Garlington W, Hiscott PS, Sheridan CM, Grant MB, Forder JR. Labeling of stem cells with monocrystalline iron oxide for tracking and localization by magnetic resonance imaging. Microvasc Res 2009; 78: 132-139.
[20] Schmidt A, Ladage D, Steingen C, Brixius K, Schinköthe T, Klinz FJ, Schwinger RH, Mehlhorn U, Bloch W. Mesenchymal stem cells transmigrate over the endothelial barrier. Eur J Cell Biol 2006; 85: 1179-1188.
[21] Stolzing A, Scutt A. Effect of reduced culture temperature on antioxidant defences of mesenchymal stem cells. Free Radic Biol Med 2006; 41: 326-338.
[22] Sotiropoulou PA, Perez SA, Salagianni M, Baxevanis CN, Papamichail M. Characterization of the optional culture conditions for clinical scale production of human mesenchymal stem cells. Stem Cells 2006; 24: 462-471.